A generalized Wagner method for three-dimensional slamming

O.M. Faltinsen [*]
oddfal@marin.ntnu.no

M.Chezhian [**]
muthu.chezhian@dnv.com

* Centre for Ships and Ocean Structures, NTNU, Trondheim-Norway
** Dept. of Marine Technology, NTNU, Trondheim – Norway

There is a broad variety of important impact problems in ship, ocean and coastal engineering. Two-dimensional problems have been extensively studied and there is a need to further develop three-dimensional theoretical methods. A somewhat special scenario is accidental drops of pipes from a platform. One concern is subsequent impact between a pipe and risers. The pipe can enter the free surface with any orientation. The flow will separate at some stage and leave a finite length cavity behind the pipe. The cavity will then collapse and the pipe can be considered fully wet in the subsequent motion in the water. The fully wetted phase has been studied by Friedman et al. (2003).

Our studies are relevant for the impact phase before flow separation occurs. However, the original motivation for our studies was 3D ship slamming. We assume irrotational flow of an incompressible fluid. A rigid body is first considered. A generalized Wagner method is followed. This means the exact body boundary condition is satisfied in combination with the outer flow free surface conditions used by Wagner. A boundary element method is used to solve the problem at each step. Theoretical slamming studies for axisymmetric bodies (e.g. Miloh, 1981, Faltinsen and Zhao, 1996) were important verification tests.

When solving the boundary value problem, the dynamic free surface condition $\phi = 0$ was applied on the quasi-horizontal plane emerging at the intersection line between the free surface and the body surface. This quasi-horizontal plane is referred to as the elevated free surface. In case of an axisymmetric body, the elevated free surface would be a horizontal plane. For an arbitrary three-dimensional body, the elevated free surface will no longer be a plane but a curved surface, which runs on a series of connecting lines. These connecting lines emerge from the intersection of the body surface and the free surface and are aligned parallel to the horizontal plane, as shown in Figure 1.

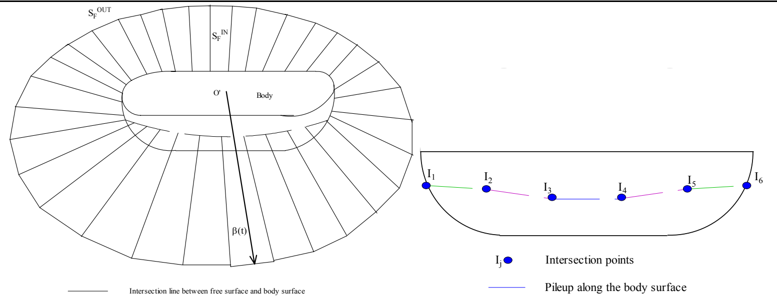

Figure 1: *Elevated Free Surface around the three-dimensional test section*

The three-dimensional outer flow solution was matched with an analytical solution form far away from the impacting body as well as a local two-dimensional solution at the body-free surface intersection, so as to calculate the exact duration between subsequent time steps. The local solution matching technique was based on the work of Zhao et al. (1996). This local solution ensures that the flow singularity at the intersection of body surface and free surface is properly accounted for in the time integration. For a general three-dimensional body, control sections are defined along which the free surface elevation is followed in time. An iterative approach was used in combination with the local solution matching and interpolation was used between the control sections to generate the wetted surface profile around the body.

The time stepping procedure and the methodology for calculating the free surface-body intersection for an arbitrary 3D geometry can be understood by studying two other basic problems, i.e. the impact of an axisymmetric body (Faltinsen and Zhao, 1997) and of a 2D asymmetric body (Zhao, Faltinsen & Aarsnes, 1996).

Consider a two-dimensional asymmetric body as given in Figure 2. The superscript notation, *r* denotes *'right side'* of the body and the superscript notation, *l* denotes *'left side'* of the body. Since the body is asymmetric, the pile up of water on either side of the body will not be the same. It is here neglected the possibility of ventilation on the left side. The same rate of change of intersection point with time *(dc/dt)* from the previous time step, is also used for the subsequent time step to get a first estimate of the horizontal line L_{i+1} (elevated free surface). In this, it is assumed that the geometry does not change rapidly, so that the above approximation can be used.

The numerical simulation starts at time instant t_0, where the submergence of the body is z_1^0. It is assumed that the free surface elevation is unaffected by this z_1^0 penetration and the free surface l_0 is horizontal. This is denoted as time step 1. At the time step 2, it is assumed that the free surface elevation is still horizontal and its above the z_1^0 at a position governed by the number of time steps we choose in the numerical simulation. The reason for doing this is to get a preliminary estimate of *(dt/dc)* which is applied in the subsequent time step.

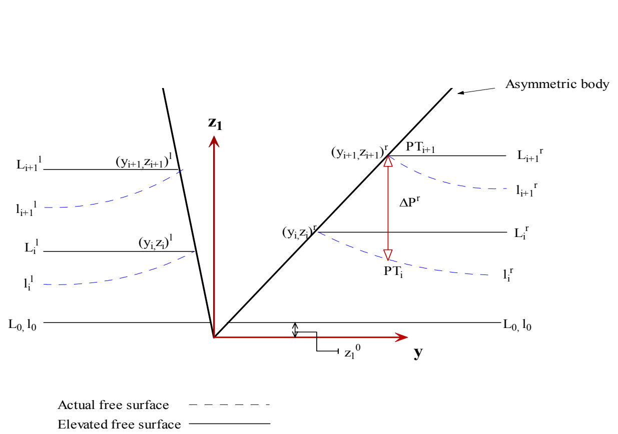

Figure 2: 'S*implified method*' *for an asymmetric 2D body showing actual free surface (____ solid line) and elevated free surface (------ dashed line).*

The subsequent time steps are dealt with as follows. The time interval for each time step is found from the right hand side of the body and the position of the intersection point for subsequent time steps is fixed for the right hand side of the body. The *(dt/dc)* of the previous time steps is combined with the 3D outer flow solution to determine the position of the intersection point on the left side of the body. Green's second identity is applied at L_i for time step t_i and at L_{i+1}^a for t_{i+1}. It should be remembered that L_{i+1}^a is obtained as a first approximation from *(dt/dc)* of the previous time step. An iterative procedure is then applied, to find the correct position of the intersection point on the *'left side'*. The kinematic free surface condition is used on the remaining part of the free surface to find out the free surface elevation.

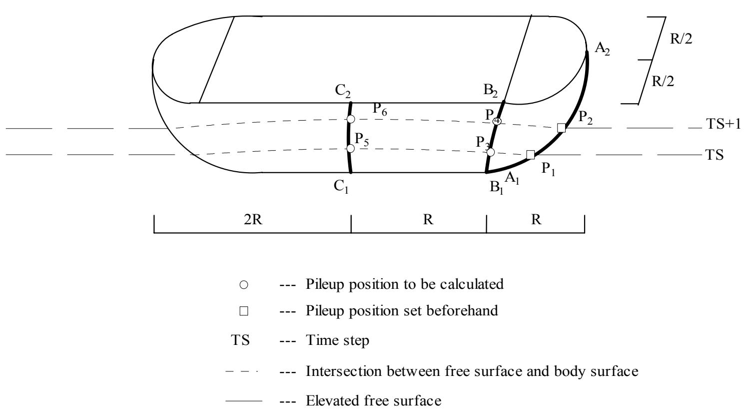

Figure 3: *Control sections and free surface intersection positions for two subsequent time steps.*

Consider a three-dimensional body as given in Figure 3. A procedure similar to the asymmetric water entry problem is then adopted. The main difference is that the section AA_1 is representative of the right hand side of asymmetric body and all other sections are representative of the left hand side of the body. For the given 3D body, the control sections are chosen at A1A2, B1B2, C1C2. As before, A1A2 is set as equivalent to the *'right side'* and section A1A2 is used to determine Δt for the time stepping process. An approach similar to that of the *'left side'* of the asymmetric body is applied for section B1B2 and C1C2. P_1 and P_2 are the predefined points that are set beforehand. P_1 corresponds to y_i^r and P_2 corresponds to y_{i+1}^r. P_3 and P_5 correspond to different y_i^l and P_4 and P_6 correspond to their y_{i+1}^l respectively. The pile-up position, i.e. the intersection line between free surface and body surface, that lies between P_2 ,P_4 and P_6 is interpolated by a second order polynomial interpolation scheme.

Since the body has two planes of symmetry, the control points A1A2 , B1B2 and C1C2, were found to be sufficient. For the given body shape, convergence was obtained with the three control sections, described above. On the contrary, a choice of larger number of control sections resulted in larger iteration time, for a given accuracy.

It should be noted that the pile-up of water on either side of a 2D asymmetric wedge section is only slightly different, even when the angle subtended by wedge surfaces to the horizontal vary by around 30 degrees. In case of a three-dimensional body, there is a gradual variation in the pile-up height around the body section. The choice of positions of the control sections such A1A2, B1B2 and C1C2 should be based on observation as well as rigorous testing. The general guideline being, more control sections should be included at places where the curvature of the body in the horizontal plane changes significantly.

Drop tests were carried out at the Model Basin in Trondheim. The test model is composed of 4 smaller sections, (indicated as I, II, III, IV in Figure 4). Vertical force, wetted surface elevation at key control sections, and pressure time history were recorded. The drop tests were performed on calm undisturbed free surface and the tests were repeated to check for reproducibility and consistency. The effect of relative velocity between the body and the water was studied, by changing the drop height, which implicitly governs the water entry velocity. The drop tests were conducted with two different trim angles (0^o and 10^o) to study the influence of the relative angle between free surface and body surface.

Part of the impact model sections were modified to provide access for mounting and shifting the pressure cells, which later turned out to be a potential source of problem due to weakened test sections. The results from the model tests were used to validate the proposed numerical method and also provided adequate information for gaining better physical understanding of the slamming phenomenon.

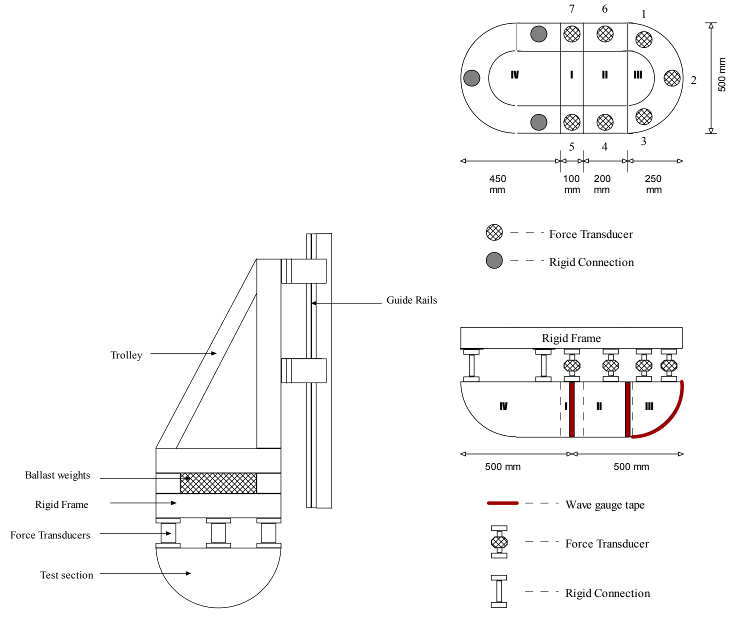

Figure 4: *Drop rig with the test section details*

The results based on numerical simulation were compared with the experimental results and overall agreement was found to be good. The vertical force from individual test sections was compared and the total vertical force on the entire model was also compared. The non-dimensional vertical force on the center section (indicated as section II in Figure 4), is shown as an example in Figure 5. The agreement with respect to rise time to peak load and the maximum vertical force was found to be good. The later part of the vertical force history showed deviations mainly due to the lack of the hydrostatic component in the numerical method and is also partly due to the non-constant vertical velocity. The presence of the oscillations in the measured experimental forces cannot be ignored.

Comparison between numerical and experimental pressure measurements and wetted surface profiles were done and possible reasons for the minor deviations was documented. The experimental pressure measurements are strongly dependent on the pressure cell diaphragm area, and the pressure cells used had a diameter of 4mm. Since the pressure peaks has a smaller spatial extent than the pressure cell area, the experimental results miss out the exact maximum. For the pressure cells located along the cylinder bottom line, the presence of the air cushion will reduce the pressures in the experimental readings.

A simplified estimate of the experimental error due to the large diaphragm area associated with 4mm diameter was done, by comparing with a similar 2D water entry problem of circular cross-section. The comparison between the pressure values based on peak pressure and the space-averaged pressure (analogous to the experimental pressure) revealed that the theoretical peak pressure can be at the most 11% more than that of the space averaged pressure. Another important reason could be the presence of the oscillations in the measured pressures. Experimental and theoretical investigations of the oscillatory experimental forces, later confirmed that indeed these oscillations were hydroelastic.

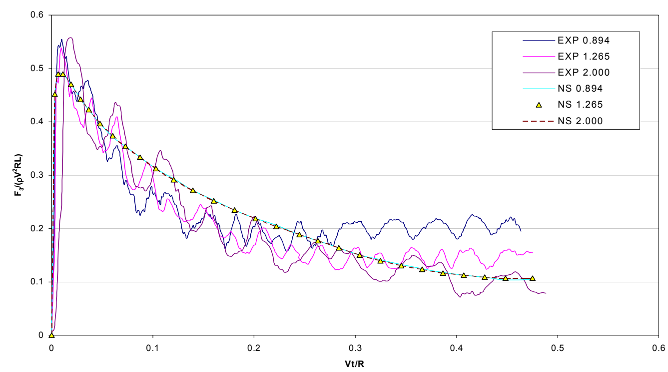

Figure 5: *Non-dimensional Vertical force on center section presented as function of non-dimensional time. No trim case. (EXP= Experiments; NS= Numerical Simulation and EXP 2.000. implies Experiments with* $V/\sqrt{gR}$ =2.000*)*

The effect of the trim angle (the relative angle between the free surface and the body surface) is also an important factor that influences slamming loads. To study the effect of trim angle, the sectional forces were systematically compared, for varying drop heights. Here again, the peak value of the oscillatory experimental force was used for comparison. Both experimental and numerical results are presented for the center sections in Figure 6. For the center section, increasing the trim angle increases the forces marginally for the 0.1m drop height. But for drop heights 0.2m and 0.5m, the forces reduce considerably. The numerical vertical force at 0.5m reduces by 30%. The reason for this difference is the flow pattern and also the entry velocity. For the 0^o trim case, the flow was close to 2D, due to the symmetric nature of the body geometry and the symmetric water entry. For the 10^o case, the flow is largely affected by the flow moving in from the end section towards the center section. Further, for the 0^o trim, the entire center section made contact with the free surface at the same time instance. For the 10^o trim, the bottom of the center section makes contact sequentially, i.e. the entire section is not wetted at the same time instant. For the 0.5m drop height the water entry velocity was not constant and there is a minor deceleration, due to the large impact force on the end section, which makes the first contact with the fluid surface. The relative velocity between the fluid and the center section becomes smaller as compared to the no trim case for 0.5m drop height case, partly leading to a smaller maximum force.

For the mid section, the force reduction is much more substantial and the force reduces for all drop heights. At 0.5m drop height, the experimental force reduces by 47%, when the trim is altered from 0^o to 10^o. The end section exhibits similar trend like the center section. The experimental vertical force for 0.5m drop height test case, reduces by, as much as, 48%, when the trim becomes 10^o. The numerical simulation also predicts the force to be halved when the trim becomes 10^o.

Miloh (1991) studied the oblique water entry problem of a rigid sphere and concluded that the presence of a horizontal velocity component always tends to reduce the maximum vertical slamming loads. These conclusions along with the results shown above for the 10^o trim case, clearly demonstrate that slamming forces are largely influenced by the local deadrise angle and the position of the initial contact. Even for small changes in trim angles, the force reduction can be significant.

Alternate ways of assessing three-dimensional water entry loads using strip theory models or simplified added mass models with von Karman type approach have also been investigated. It was found that strip theory overestimates the vertical force for all drop test cases for the total body. For 0.1m test case, the deviation of the strip theory from experimental results is significant, whereas for 0.2m test case, the strip theory solution moves closer to experimental results and for 0.5m drop case, it even compares better. The relative error for the peak value of strip theory and experimental mean trend line for 0.1m drop test is larger than for the 0.5m drop case. This indicated that with increasing entry velocity, the strip theory predicts the three-dimensional forces with better agreement. This implied that the basis and assumptions for strip theory approximation, seem to become more valid with the increasing water entry velocity. For the hemispherical end section, the strip theory gave poor predictions, and the deviation in the peak force was as large as 30% when compared to the experimental peak force, reinstating the significance of three-dimensionality.

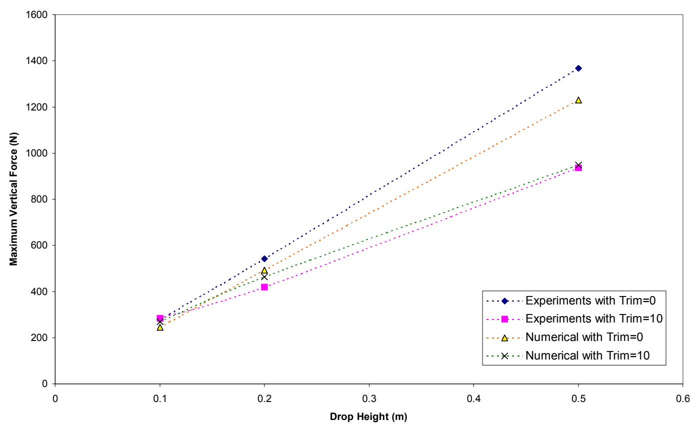

Figure 6: *Maximum vertical force on center section. Effect of trim angle.*

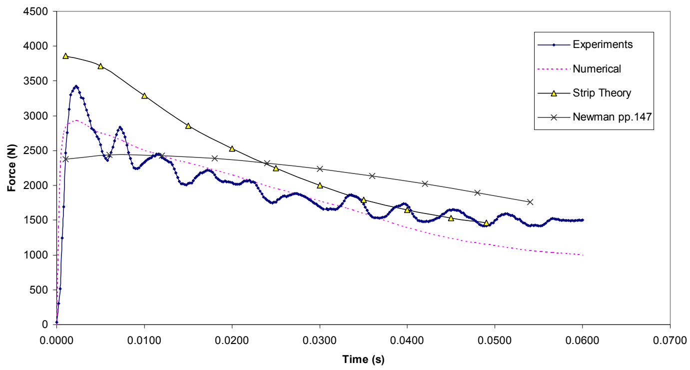

Figure 7: *Total vertical force using strip theory and von Karman type approach for 0.2m drop height. No trim case.*

The experimentally recorded vertical forces showed an oscillatory trend, which was missing in the numerical method based on assuming a rigid body. After thorough investigation using dry impact hammer tests and finite element analysis using FEMLAB, the source of the oscillations were ascertained to be from the hydroelastic vibrations of the test sections. Simplified 2D hydroelastic models were proposed and implemented using the thin beam theory approximations. Two different hydroelastic studies have been carried out on the center section. The first study modeled the center section as 3 connected beams, with space averaged vibrational velocities on the lower horizontal beam. Since good quantitative agreement could not be achieved, a further refinement of the 3-beam model was attempted using velocities described by a Fourier series representation. These investigations confirmed that hydroelasticity was source of the oscillations in the experimental force curves. Though good qualitative agreement has been documented, the low quantitative agreement was further studied. The test model construction and composition, model defects and flaws introduced due to weakening of the sections to mount/shift pressure cells, were found to be the main reason for deviations.

Guidelines are needed for future model tests, where such errors can be minimized, so that three-dimensional rigid body force can be assessed and compared with better accuracy. The ideal test model should have very low mass and high stiffness. Low mass is required, so that the inertial forces can be small and the force transducers can record the actual slamming force. High stiffness is required, so that the model behaves like a rigid body and the hydroelastic effects and dynamic effects can be reduced. It is suggested that a simple FEM model is generated and analyzed, so as to identify the eigen frequencies which can be problematic later. This can be used to improve the model qualities and low frequency oscillations can be avoided, by choice of appropriate composite materials.

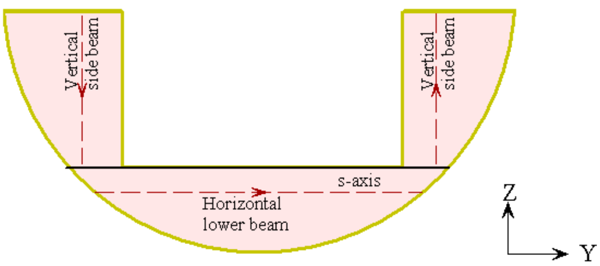

Figure 8: *Three beam model*

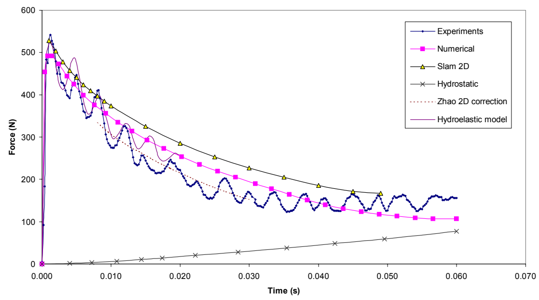

Figure 9 : *Results based on three-beam hydroelastic space averaged velocity model.*

References

FALTINSEN, O.M., ZHAO, R. (1997). Water entry of ship sections and axisymmetric bodies, AGARD, *High speed body motion in water*, Kiev, Ukraine.

FRIEDMAN, A., ZILMAN, G., MILOH, T. (2003). Dynamics of a body falling in waves, *18th Int. Workshop on water waves and floating bodies*, Le Croisic, France.

MILOH, T. (1991). On the oblique water-entry problem of a rigid sphere, *J. Eng. Math*., Vol. 25, pp. 77-92.

MILOH, T. (1981). Wave slam on a sphere penetrating a free surface, *J. Eng. Math*., Vol. 15, No. 3, pp. 221-240.

ZHAO,R., FALTINSEN, O.M., AARSNES, J.V. (1996). Water entry of arbitrary two-dimensional sections with and without flow separation, *21st Symp. On Nav. Hydrodyn,* Trondheim, Norway.